ATLID Beam Steering Mechanism and derived new piezoelectric based devices for optical applications

F. Bourgain[(1)], F. Barillot[(1)],C. Belly [(1)], F. Claeyssen
[(1)] Cedrat Technologies S.A., MEYLAN, FRANCE, Email:actuator@cedrat-tec.com

ABSTRACT

In Space & Defence (as well as in many others fields), there is a trend for miniaturisation in active optics requiring new actuators. Applications also often require the ability to withstand high vibrations and shocks levels, as well as vacuum compatibility for space applications. A new generation of small and smart actuators such as piezoelectric (piezo) actuators, are resolving this trend, thanks to their capacity to offer high energy density and to support both extreme and various requirements. This paper first presents the BSM mechanism and its requirements, the technologies involved in the design and the validation campaign results. Secondly, a derived XY piezoelectric positioning stage based on the same APA® and associated Strain Gage sensing technology is presented with its associated performances. Finally, a new piezoelectric motor based on the APA® technology, which allows the combination of long stroke while maintaining high resolution positioning of optical elements, is presented with experimental performances.

Keywords: Piezo, Mechanism, Tip-tilt, Stability, Strain gages

1. INTRODUCTION

BSM Mechanism context

ATLID (ATmospheric LIDar) is one of the four instruments of EarthCARE, it shall determine vertical profiles of cloud and aerosol physical parameters such as altitude, optical depth, backscatter ratio and depolarisation ratio.

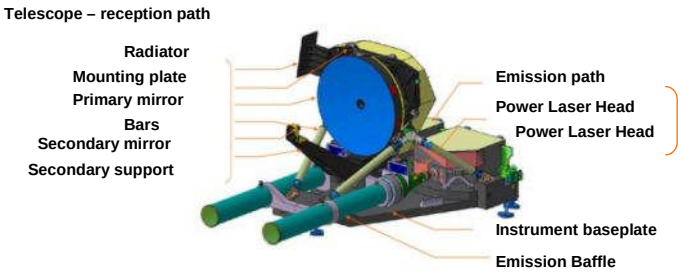

Figure 1: ATLID Instrument overview [1]

A new tip tilt mechanism based on low voltage piezoelectric actuators has been designed by Cedrat Technologies to answer the high level of stability required for the Earthcare satellite. The Beam Steering Assembly aims to deviate a pulsed high energy UV laser beam to compensate for misalignment between the emission and reception paths of ATLID [1] with a very high stability and resolution.

The BSM is a range pointing mechanism, implemented in Power Laser Head Optical Bench, inside the pressurized PLH. See Figure 2.

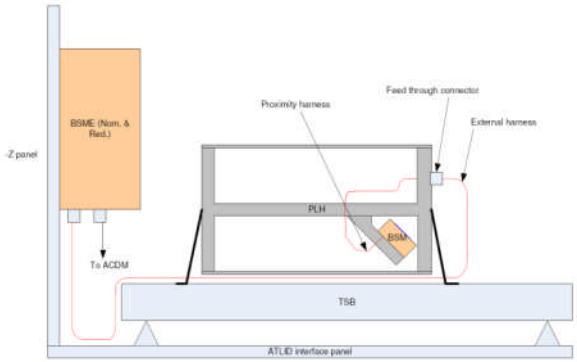

Figure 2 : BSA implantation schema

Mechanism description

The BSM is composed by 2-axis Tip-Tilt mechanism (TTM), mounted on a bracket, see Figure 3. The BSM is based on two stiff push pull pairs of APA60S-NM® actuators [2] equipped with Strain Gages (SG). The basic principle is to convert translation movement produced by APA® into rotation trough pivots and cardanic joint, see Figure 4.
This design allows a mechanical resonant frequency above 2kHz thus avoiding the use of a launch locking mechanism and limiting the micro-vibration susceptibility.

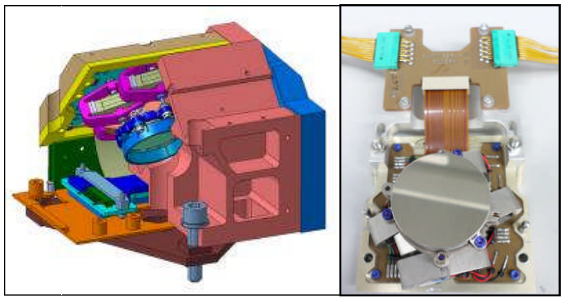

Figure 3: BSM: a-CAD view of BSM b-TTM stand alone

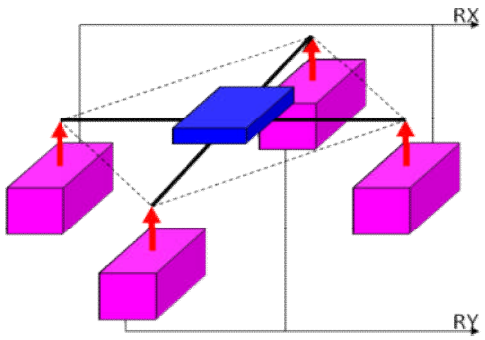

Figure 4: TTM principle

The BSM is required to steer the incoming laser beam through a range of +/-2.12mrad for Rx rotation and +/-1.5mrad for Ry rotation (Mechanical Angle) with a bandwidth up to 10Hz.
To achieve this stroke dissymmetry using the same voltage profile, the distance between APA® on the 2 axis is different. This choice enables maximisation of the applied voltages on the piezo ceramics and hence improves the overall sensitivity of the mechanism.

Performances and mechanism behaviour have been simulated and validated with FEM. The justification design followed ECSS safety margins.

2. QUALIFICATION CAMPAIGN

The qualification campaign has been done on the EQM, prior to the realization of Flight models.

A specific Ground Support Equipment (GSE), based on standard products from Cedrat Technologies, is used for Piezo driving, Strain gages signals conditioning, and Closed loop control (digital controller).
A test bench using an autocollimator in a control temperature environment has been used (Figure 5).

The autocollimator is configured in differential mode. It means that the results of the measurement are the difference between the reference mirror angle and the TTM mirror angle. This method minimises the error from the parasite angle from the reference plate and thermo-mechanical influence of the test bench.

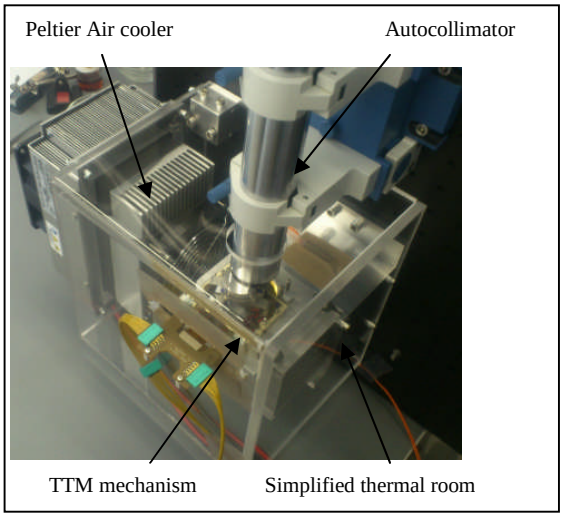

Figure 5: Test bench supporting the BSM for the qualification campaign

Tests sequences

The campaign followed the next steps (Figure 6). Levels are different depending on tested model: more stringent on the QM than FMs.

Tests description	QM	FM1&FM2
Thermal vacuum stowing (+65°C)	TTM	TTM
Properties verification tests: 1. Physical properties 2. Electrical properties	 BSM BSM	 BSM BSM
INITIAL functional and performance burn-in test at ambient	TTM	TTM
Mechanical environment tests: 1. LSRC (Low Sine resonance characterization) 2. Quasi-static 3. LSRC 4. Sine 5. LSRC 6. Random 7. LSRC	 TTM TTM (Q) TTM TTM (Q) TTM TTM (Q) TTM	 N/A
INTERMEDIATE functional and performance burn-in test at ambient	TTM	N/A
Non operational thermal cycles (storage)	TTM (Q)	N/A
INTERMEDIATE functional and performance burn-in test at ambient	TTM	N/A
FINAL functional and performance burn-in test at ambient	TTM	N/A

Figure 6**:** Performed tests on QM, FMs

A few results are detailed further.

Resonant frequency:
Results on resonant frequency are obtained using an impedance analyser HP4194A. Each rotation axis is analysed separately.

The consistency of mechanical behaviour can be seen comparing resonant frequencies of different produced mechanisms.

Phase	Rx (Hz)	Ry (Hz)
EQM	2451	2882
FM1	2476	3070
FM2	2439	3178

Table 1: Summarise of measured mechanical resonant frequency on 3 manufactured mechanisms.

One critical aspect during the qualification campaign was the withstanding of the mechanism to vibrations during launch (15.5 G rms). To evaluate the mechanism behaviour, we compared initial RFR and RFR after sinus and random vibrations (see Figure 7). The first mode stayed within specified range, the slight change in amplitude and position is caused by screws micro-sliding. All performances (stroke, resolution…) remained compliant with the requirements.
This point led to an additional vibration settling after mirror integration prior to launch, in order to keep the mirror centre at the same position after launch.

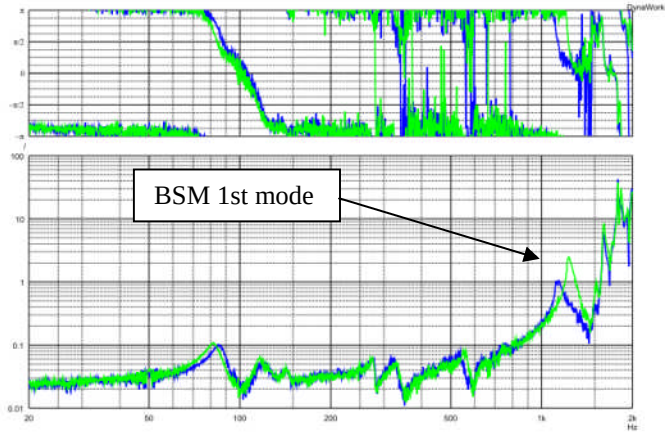

Figure 7: Resonant frequency research (in blue initial, in green final)

Closed-loop displacement:
Very small measurements are difficult to measure using conventional apparatus. The autocollimator reaches its resolution limitation when sub-mrad motions are required. Full stroke displacement shows linearity below 1.4% for Rx and 1.2% for Ry (Fig. 10).

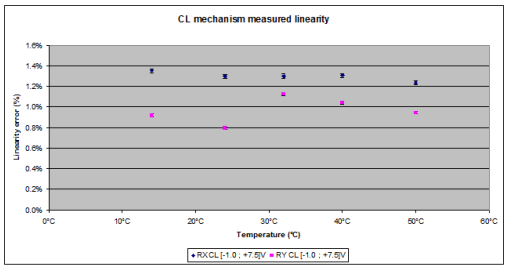

Figure 8: Closed-loop linearity of full stroke displacement on Qualification temperature range

Repeatability:
Mechanism interest performance is also conditioned by good repeatability. The reached positions after several On-Off sequences are compared and the worst difference is considered on five On-Off cycles.
Results are showing repeatability better than 10µrad on both axes between the qualification temperature range. Repeatability of 0° Mechanical position is always better than 2µrad for temperatures up to 40°C. These results are presented in Figure 9 .

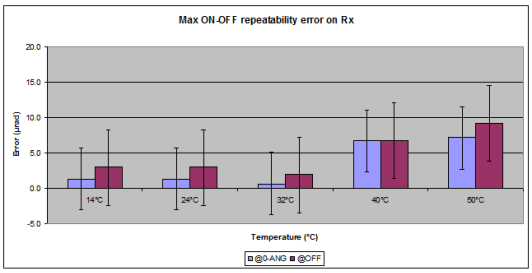

Figure 9**:** Repeatability results on Rx axes on Qualification temperature range

Thermal sensitivity:
Position 0° mechanical angle is followed throughout the temperature range. This gives thermal sensitivity of the mechanism around both axes. It is seen that in Closed-loop, thermal sensitivity is below 3.2µrad/K for Rx and 0.8µrad/K for Ry. Results are visible in Figure 10.

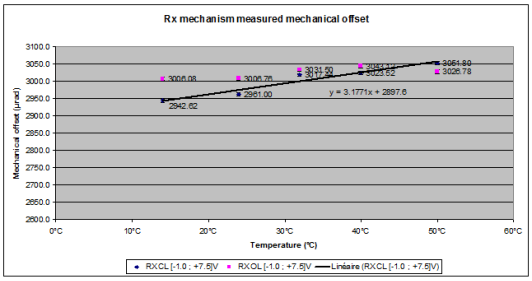

Figure 10**:** 0°Mechanical angle along temperature range for Rx

XY piezo stage

An XY mechanism (see Figure 11) is designed using the shape of an APA®. The moving frame, including actuators, is monolithic.

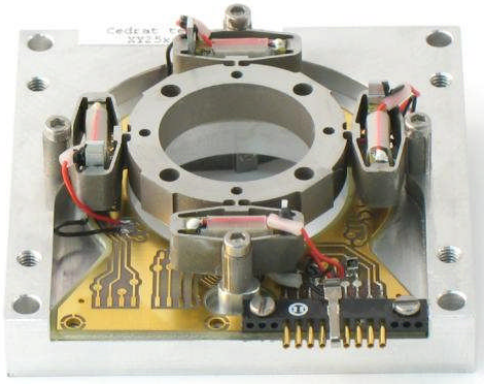

Figure 11: XY25XS stage view

The stroke is computed using FEM (see Figure 12), as well as stresses resulting from integration, thermal environment, vibration/shocks capability. All the stress contributions were summed for both non-operational and operational modes to validate the overall reliability of the mechanism.

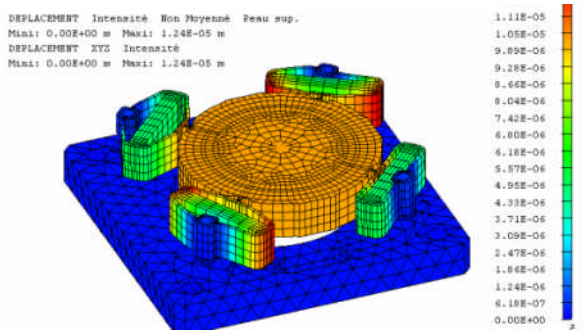

Figure 12: Stroke simulation example

Several performances verifications have been made, such as stroke, cross coupling, repeatability, parasitic displacement, thermal behavior, closed loop performances.
A few results are detailed further.

Stroke:
The stroke on both axis has been measured in open loop, explaining the hysteresis coming from the piezoelectric component (see Figure 13). This hysteresis is cancelled using closed loop control based on SG feedback (for low frequencies).

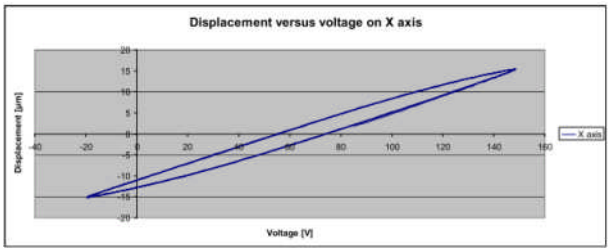

Figure 13: Open loop stroke

Performance in closed loop:
For both axis, the error between the driving signal and integrated SG at 30Hz for a ±9µm order is less than ±50nm (<0.6%), and the error at 100Hz for a ±2.7µm (<5%) order is less than ±125nm.

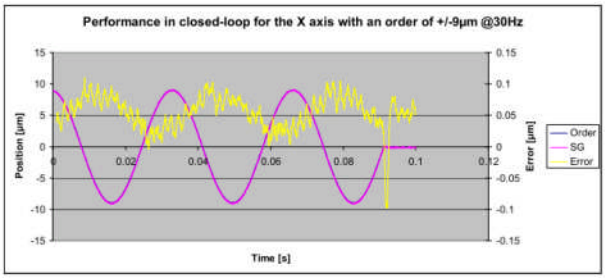

Figure 14: Comparison of order and SG response under +/-9µm @30Hz.

Parasitic displacement:
The measured parasitic rotation is slightly less than ±40µrad for both axis on the complete stroke.
As expected, the actuation on the X axis mainly creates a parasitic rotation around the Y axis (Rx), and the actuation on the Y axis mainly creates a parasitic rotation around the X axis (Ry).

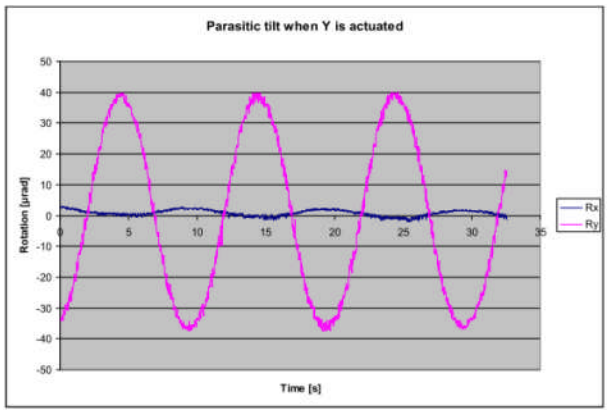

Figure 15: Parasitic tilt when Y is actuated

On the Oz axis, the parasitic displacement Tz is under +/-100nm.

For both axis, the error between the driving signal and integrated SG at 30Hz for a ±9µm order is less than ±50nm (<0.6%), and the error at 100Hz for a ±2.7µm (<5%) order is less than ±125nm.

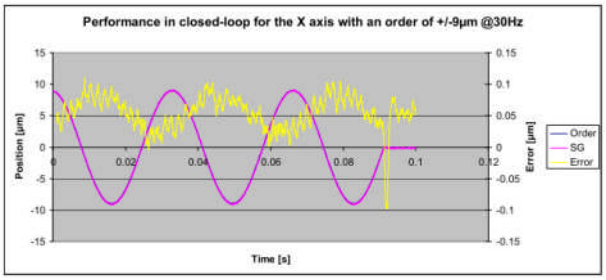

Figure 16: Comparison of order and SG response under +/-9µm @30Hz.

Cross coupling:
When the mechanism is actuated following X axis, due to the monolithic frame the displacement following the Y axis in not null (see Figure 17) .
The range for cross-coupling is ±25nm for both axis. The SG are able to read the cross-coupling effect, which means that this effect will be compensated in closed-loop.

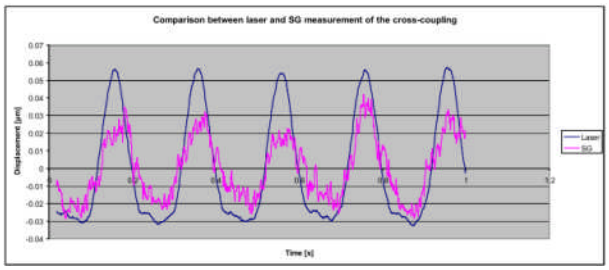

Figure 17: Cross-coupling visualisation

Piezoelectric motor

APA® shape is also offering benefits within piezo motor configuration [3]. Amplification and preload are key points that lead to obtain good stepping motor characteristics. Stepping Piezo Actuators (SPA) Stepping Piezo Actuators are inertial stepper motors. They are composed of four main elements: an actuator, a shaft, a mass and a clamp. The principle of such motors is simple and relies on stick-slip effect and dissymmetrical accelerations. Figure 18 shows the two phases

needed to produce one step. First, a slow contraction of the actuator makes the mass moving, without any motion of the shaft, because of clamping friction. Then, a fast actuator expansion gives dynamic forces to mass and shaft and, because of the inertia of the mass, overcomes the friction forces. This moves the shaft into the clamp and one step is completed. By repeating this operation, stroke of several millimetres can be reached. The opposite motion is done by inversing the two sequences. This motion is called “Stepping Mode”.

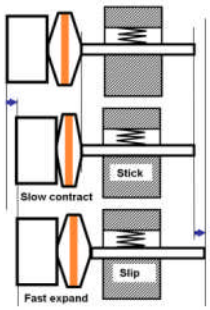

Figure 18: SPA Motor principle

Linear and rotating configurations have been developed, targeting camera refocusing, long stroke shutters or even medical applications. An innovative realization is presented here, that can achieve very high resolution positioning while offering survivability to extreme loadings.

Overall presentation:
The presented motor is based on a rotating motor coupled to a linear/rotating conversion system. Proposed prototype is 50 mm in diameter and 63mm high, for 260gr weight. Its stroke is 1mm and it is able to produce more than 200N force. Figure 19 shows the considered prototype.

Figure 19: High resolution motor

The internal structure allows decoupling high external forces from actuation mechanism. This configuration makes the motor compatible with high load and high levels of vibration. The proposed configuration is built to support 1.8kN axial force without losing its locked position.

Motor resolution:
In order to prove motor resolution, step by step signal is applied and position output is controlled using capacitive sensor. Those sensors are facing output axis of the motor, with a 50µm/V gain. Acquisition is made using a National Instruments acquisition board, with adapted generation/acquisition Virtual Instrument. Signal generation is performed using same device.
Figure 20 presents results obtained on motor, using a 75Vpp signal @ 1Hz. Resolution of steps below 20nm is shown. This corresponds to a 1.2µm/min speed. Speed reached with a 20Hz and full voltage amplitude signal (150Vpp) is 75µm/min.

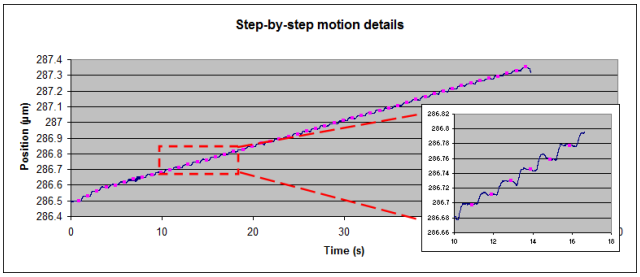

Figure 20: Motor stepping acquisition, mean step size is about 20nm.

Short terms lifetime testing:
Some very resolute application can be seen is optical fine tuning, and/or structure deformation apparatus. Those kinds of application can (but are not limited) be performed in a very limited actuation number. A short lifetime actuation test has been performed at maximal voltage amplitude. 110 back and forth actuations have been performed showing following behavior (see Figure 21).

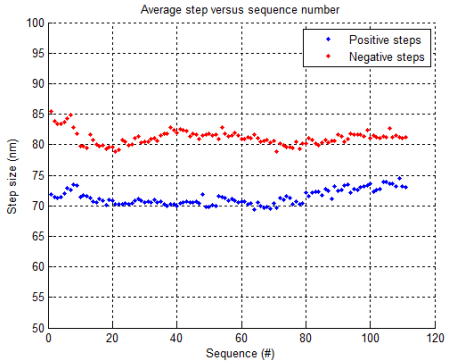

Figure 21: Cycling test results

Constant step size is shown along cycles, with a small variation. Dissymmetry of step facing direction (classical in stepping piezo motor) is also visible, but is not an issue in piezo motor field.

3. CONCLUSION

These mechanisms show the pertinence of the use of APA® with Strain Gage technology for demanding applications.

APA actuators can also be employed within piezo motors. Proposed configuration shows high resolution (below 20nm) with large force compliance.

REFERENCES

[1] Hélière, A. , Gelsthorpe, R., Le Hors, L., Toulemont, Y., “ATLID, the atmospheric LIDAR on board the EarthCARE satellite,” ICSO, (2012)

[2] Barillot, F., Fabbro, H., .Le Letty, R. , Guay, Ph., “Design and tests of normally centred piezo mechanisms and their control electronic,” 10th European Space Mechanisms and Tribology Symposium, (2003)

[3] Belly C., Charon W., “Benefits of amplification in an inertial stepping motor,” Mechatronics 22, 177-183 (2012)